Results in Engineering 19 (2023) 101246

Contents lists available at ScienceDirect

Results in Engineering

journal homepage: www.sciencedirect.com/journal/results-in-engineering

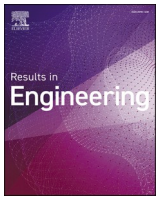

Modification of perforated plate in fluidized-bed combustor chamber through computational fluid dynamics simulation

Erdiwansyah [a,d,e], Mahidin [b,**], Husni Husin [b], Nasaruddin [c], Asri Gani [b,f,*], Rizalman Mamat [d]

[a] Doctoral Program, School of Engineering, Post Graduate Program, Universitas Syiah Kuala, Banda Aceh, 23111, Indonesia
[b] Department of Chemical Engineering, Universitas Syiah Kuala, Banda Aceh, 23111, Indonesia
[c] Department of Electrical and Computer Engineering, Universitas Syiah Kuala, Banda Aceh, 23111, Indonesia
[d] Center for Automotive Engineering, Universiti Malaysia Pahang, 26600, Pekan, Malaysia
[e] Faculty of Engineering, Universitas Serambi Mekkah, Banda Aceh, 23245, Indonesia
[f] Research Center of Palm Oil and Coconut, Syiah Kuala University, Banda Aceh, 23111, Indonesia

ARTICLE INFO

Keywords:
Perforated plate
Fluidized-bed combustor
Modification
Computational fluid dynamics
Biomass fuel
Modelling simulation

ABSTRACT

The combustion of solid fuels in a combustion chamber can be perfect if all the fuel included can burn out, and nothing remains. The combustion chamber requires sufficient air to burn all the fuel; therefore, meeting the air supply requires modifications with various considerations. The perforated plate modeled through computational fluid dynamics (CFD) was modified to investigate the excess air supply into the combustion chamber. The CFD simulation modeled in this study was used to validate the results of the experiments carried out with the previous fluidized-bed combustor technology. The simulation results show that the temperature increased for all fuels tested in geometry-2 compared with geometry-1. The best boiler efficiency from the simulation results is in geometry-1 for 45% oil palm midrib fuel with a mass flow rate of 7.78 kg/s. The maximum radiation was recorded from geometry-2 at a variation of 66.939 W/m^{2,} with a heat loss level of 1.10 W/m^2. Overall, the simulation was performed by modifying the fuel floor plate in geometry-2 to increase the temperature and radiation with lower heat loss.

1. Introduction

Heating energy derived from biomass has been used for cooking and the main ingredient since ancient times. This is because their use and availability worldwide have different and abundant diversity [1–3]. Recently, the interest in using biomass as an alternative to fossil fuel energy has increased significantly. Solving solid biomass combustion for heating and power generation has attracted considerable interest. This is because several industries are trying to find energy-saving solutions by utilizing energy from biomass waste [2]. The demand for biomass pellet fuel continues to increase along with global warming from greenhouse gas emissions. However, there is a lack of interest in renewable fuels derived from biomass because they have a high ash content [4]. The results of this study show that the ash content can be reduced by up to 1% through torrefaction with a temperature of 180 °C.

The combustion of solid biomass has several problems, particularly obstacles to the transition to energy sources. However, burning solid biomass has been considered to reduce the emission of carbon dioxide and pollutants that can harm human health (such as PM and NOx) [5,6]. In addition, inorganic compounds and alkali metals in the biomass composition cause corrosion and ash in the biomass combustion system. A high content of alkalis, such as potassium and sodium, reduces the melting point of the ash. Condensation of inorganic vapors on the surface during heat exchange is the starting point for forming an impurity layer. The reduced fusion temperature can promote slag formation on the characteristics in direct contact with the fuel bed [7,8]. The decrease in the thermal efficiency of the combustion system is caused by slagging and fouling, which also results in system damage [9–11].

These problems can be reduced using several techniques, and their use in the future is more attractive and provides more significant benefits, especially for heating and power generation. Immediate action can be performed with a differential to affect the combustion properties directly, and unwanted phenomena can be avoided during testing. In addition, the secondary activity of filtering and treating the exhaust gas

* Corresponding author. Department of Chemical Engineering, Universitas Syiah Kuala, Banda Aceh, 23111, Indonesia.
** Corresponding author.
E-mail addresses: mahidin@usk.ac.id (Mahidin), asri_gani@usk.ac.id (A. Gani).

https://doi.org/10.1016/j.rineng.2023.101246
Received 14 February 2023; Received in revised form 10 June 2023; Accepted 17 June 2023
Available online 19 June 2023
2590-1230/© 2023 The Authors. Published by Elsevier B.V. This is an open access article under the CC BY-NC-ND license (http://creativecommons.org/licenses/by-nc-nd/4.0/).

and inhibiting fouling in the air supply hole can be reduced, and complete combustion can be achieved. Air injection and fluidized-bed combustion (FBC) temperature control is commonly used for solid fuel combustion. The air injection system used in several studies can reduce gas and PM emissions [12–16]. A low ratio of primary air can reduce PM emissions, which is influenced by the low air velocity in the FBC chamber, resulting in less elutriation [12,15]. Combustion with secondary air injection gradually helps achieve more efficient exhaust gas burnout, and NOx emissions can be reduced [12,15]. A lower primary air ratio can help lower the layer temperature when using solid biomass fuels. However, the risk of surface fouling in the presence of melted ash can be reduced [15]. Cooling and exhaust gas recirculation (FGR) techniques can reduce the bed temperature. The FGR created by alternating primary air with pre-cooled exhaust gas helps reduce oxygen concentration. Thus, the temperature at the FBC can be reduced, and the thermal conversion process can be further slowed. Studies have shown that FGR can help reduce unburned fuels such as NOx and PM emissions in the combustion chamber [17–19]. Cooling using water and cement with insulation on the walls of an FBC combustion chamber is a solution that can be used. For the middle to upper scales, a cooler can be used with water on the walls of the FBC room. A cooling system with the formation of water pipes around the FBC combustion chamber with domestic boilers can reduce PM emissions without affecting other combustion parameters, as reported by Refs. [20,21].

A small-scale combustion system tested to investigate the effect of air staging with the cooling system design in FBC was investigated by Ref. [22]. The designed cooling section is a complete cooling system that includes the entire FBC combustion chamber. The characteristics of the temperature distribution in the combustion system and pollutant emissions are possible because the factory has been equipped with thermocouples in several different parts. In addition, a gas analysis system and a low-pressure impactor were connected to the chimney [17,18]. Experimental studies have been conducted to investigate the repeatability and stability of the facility and the use and effectiveness of different air ratios. Thus, cooling FBC and FGR combustion chambers can reduce pollutant emissions [22,23].

The application of two- and single-stage perforated plates to flowmeters to measure cryogenic liquids has also recently been carried out [24]. The results of the tests show that the two-stage perforated plate with an optimized gap has a smaller pressure drop and a more horizontal flow coefficient profile than the single-stage perforated plate. The FBC's perforated plate was applied to probe the CO_2 adsorbent particles [25]. The tests' results significantly affect the particle friction induced by the presence of gas jets through the perforated plate applied in FBC. Managing fluid flow through perforated plates is appropriate for convective heat transfer applications [26]. The application of perforated plates in fluid dynamics with row-shaped perforations (n), hole diameter (d), chamfer radius (r), and pressure ratio (P_i/P_1) has also been carried out [27]. The experimental results show that the perforated plate can reduce the pressure gradient and velocity.

Analysis and investigation of solid biomass combustion can be carried out using computational fluid dynamics (CFD) software. Numerical Analysis makes it possible to deal with aspects not easily characterized experimentally. In addition, numerical tools can reduce design costs and optimize solid biomass combustion. Heat transfer, fluid flow, and homogeneous chemical reactions in the gas phase can be solved using CFD. Biomass thermal conversion models or empirical correlations with one-dimensional models can facilitate CFD incorporation owing to lower computational costs [28–30]. Numerical modeling of a combustion chamber with one-dimensional empirical incorporation can improve air performance so that it is possible to reduce particulate matter and nitrogen oxide emissions [29,30]. However, this model could not predict the combustion phenomenon in an FBC combustion chamber. Fuel particle and thermal process characterization can be traced using Lagrangian modelings, such as the discrete phase model (DPM) and discrete element method (DEM), with the addition of solid biomass thermal conversion modeling [31–33]. Characterization through this model allows for a more realistic solid biomass combustion, which is better but has a higher computational cost.

Eulerian modeling has a lower computational cost than Lagrangian modeling. In addition, Eulerian modeling is more comprehensive than one-dimensional modeling [31]. Generally, this model defines the porous zone in the solid phase, live gas, and the adjacent freeboard. In addition, it is also used to determine simple fluidizations that allow the dynamic coupling of the two degrees [34–36]. Simulations with the Eulerian model can provide oxygen air conditions for different fuels with different scales, especially during small-, medium-, and large-scale experiments [37–39]. However, this model does not use fuel layers for the individual particles. However, physical algorithms can be implemented in simulations of the movement and compaction of fuel in a combustion chamber [40,41]. Modeling through modification of the perforated plate in the FBC combustion chamber as a supplier of excess air was applied in this study.

This study applies the CFD software to the model to validate the regularity by modifying perforated plates. This simulation investigated and validated the combustion results from an FBC combustion chamber fueled by solid waste oil palm biomass. Modeling was carried out using the FBC technology used for combustion experiments. The FBC combustion technology is applied as an experimental tool with a modification of the perforated plate, which aims to supply excess air into the combustion chamber. The temperature results generated from the simulation were compared with the experimental results of direct combustion in the FBC combustion chamber for all the cases.

2. Materials and methods

This study investigated the effect of perforated plate modification on the combustion temperature of different solid palm oil biomass fuels. The modified plates were made of three other models plus a standard plate as a reference for comparing the results obtained. The experimental data used as a reference in this study were obtained from previous research [42–44]. The fluidized-bed combustor (FBC) combustion chamber used for the experiment was made of a steel plate with a thickness of 5 mm and a height of 40 cm. Above the FBC combustion chamber, the freeboard functions as a heat sink before entering the boiler. The boiler height was 40 cm, with a total of 121 tubes with a diameter of 20 mm for each pipe. The type of mesh used in this simulation is presented in Fig. 1.

The FBC combustion chamber for this experiment was equipped with a blower fan that functioned as the air supply. Temperature data, furnace efficiency, thermal efficiency, and heat transfer rate were measured using a thermocouple and a Digital Thermometer (HotTemp HT-306). The combustion test in the FBC combustion chamber used palm oil solid waste biomass fuels such as palm kernel shell (PKS), empty fruit bunches (EFB), and oil palm midrib (OPM). Each fuel type was tested when the modification of the perforated plate and the standard scale were applied. Three types of modified plates and one standard plate were used as a reference for comparison. The combustion temperature was measured using a thermocouple placed approximately 15 cm from the floor of the fuel plate.

Computational methods for solving discrete fluid equations are known as computational fluid dynamics (CFD). The steps of the CFD process are summarized in Fig. 2.

Computational Fluid Dynamics (CFD) converts fluid dynamics flow equations in their integral and derivative forms into discretized algebraic forms. The settlement with a computer can yield flow values at a certain point or discrete time. Three flow equations in fluid dynamics exist continuity, momentum, and energy.

The calculation of the value of continuity in integral form using (**eq. (1)**).

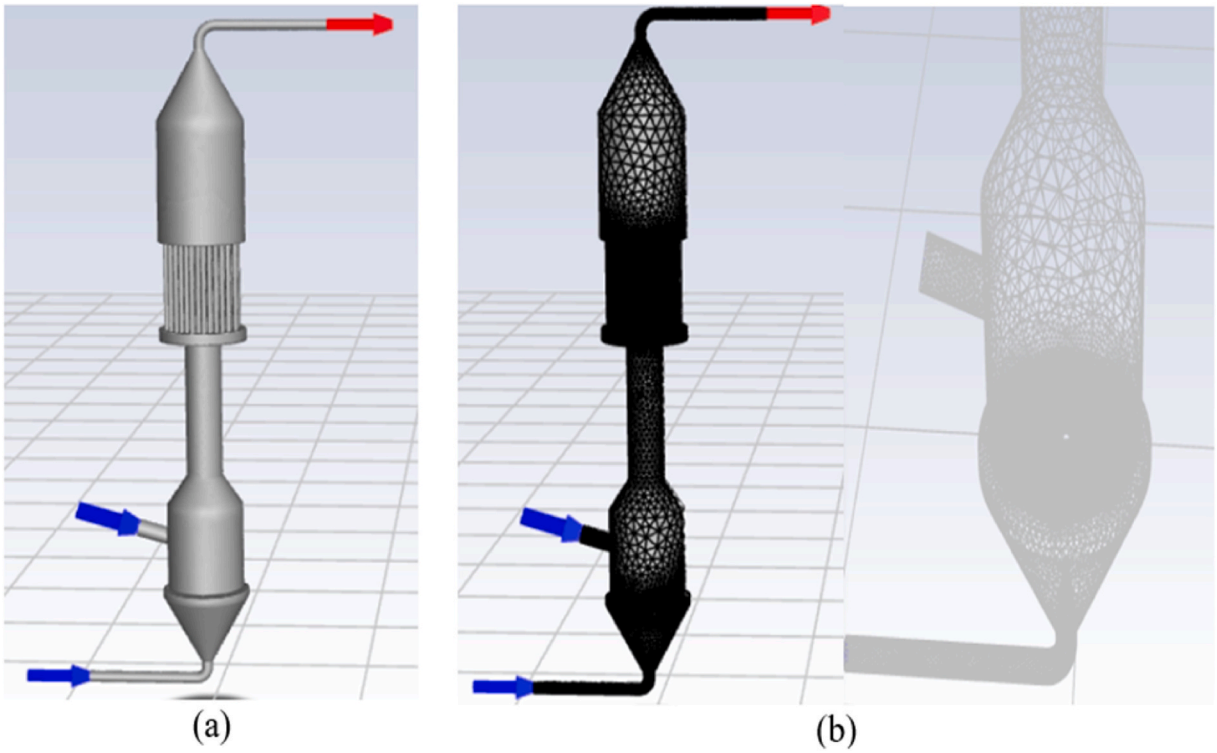

Fig. 1. (a) Type of Boiler (b) Mesh on the boilers.

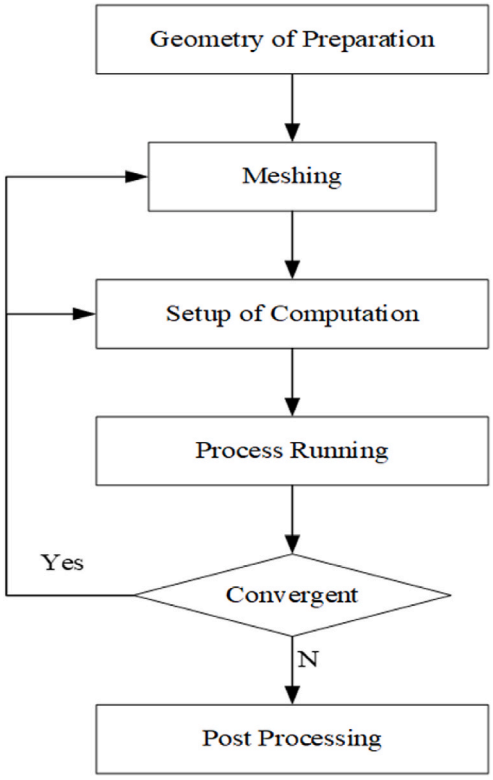

Fig. 2. CFD simulation flow chart in general.

$$\frac{\partial}{\partial t}\iiint_V \rho dV + \iint_A \rho \vec{V} \bullet d\vec{A} = 0 \tag{1}$$

Meanwhile, to calculate the value of continuity in differential form using (eq. (2)).

$$\frac{\partial \rho}{\partial t} + \rho \vec{\nabla} \bullet \vec{V} = 0 \tag{2}$$

Momentum in the x-axis direction can use (eq. (3)).

$$\frac{\partial(\rho u)}{\partial t} + \vec{\nabla} \bullet \left(\rho u \vec{V}\right) = -\frac{\partial p}{\partial x} + \frac{\partial \tau_{xx}}{\partial x} + \frac{\partial \tau_{yx}}{\partial y} + \frac{\partial \tau_{zx}}{\partial z} + \rho f_x \tag{3}$$

Meanwhile, for momentum in the y-axis direction, we can be using (eq. (4)).

$$\frac{\partial(\rho v)}{\partial t} + \vec{\nabla} \bullet \left(\rho v \vec{V}\right) = -\frac{\partial p}{\partial y} + \frac{\partial \tau_{xy}}{\partial x} + \frac{\partial \tau_{yy}}{\partial y} + \frac{\partial \tau_{zy}}{\partial z} + \rho f_y \tag{4}$$

Meanwhile, to get the momentum value in the direction of the z-axis using (eq. (5)).

$$\frac{\partial(\rho w)}{\partial t} + \vec{\nabla} \bullet \left(\rho w \vec{V}\right) = -\frac{\partial p}{\partial z} + \frac{\partial \tau_{xz}}{\partial x} + \frac{\partial \tau_{yz}}{\partial y} + \frac{\partial \tau_{zz}}{\partial z} + \rho f_z \tag{5}$$

The calculation of the energy generated in the internal form using (eq. (6)).

$$\frac{\partial}{\partial t}\left[\rho\left(e + \frac{V^2}{2}\right)\right] + \vec{\nabla} \bullet \left[\rho\left(e + \frac{V^2}{2}\right)\vec{V}\right] = \rho \dot{q} - \frac{\partial(\rho p)}{\partial x} - \frac{\partial(vp)}{\partial y} - \frac{\partial(wp)}{\partial z} + \rho \vec{f} \bullet \vec{V} \tag{6}$$

The solution of the partial differential analytical equation produces a continuous closed-form dependent variable expression in all the domains. In contrast, the solution of a numerical equation can only provide values at discrete points in the domain, also known as grid points.

2.1. Boundary conditions

The input values for the Boundary Conditions used in the simulation had three variations, as presented in Table 3. The input values at the boundary are fuel and air, supplied through pipes and entered through perforated plates modified beforehand. The perforated plate used for modeling the simulation is shown in Fig. 3. Standard plate and modified plate are the means implemented in FBC. These two plates are used as the ground floor where the fuel is used for combustion. Furthermore, the standard and modified plates are modeled via CFD, which is used for the simulation. After the modeling process, the two plates are named geometry-1 and geometry-2.

2.2. Simulation of computational fluid dynamics

The CFD method has been used in various industries, including aerospace, maritime, automotive, manufacturing, energy, renewable energy, to even bioengineering; thus, the phenomena that are worked on are also increasingly varied, so that there are no verification and validation procedures that can be used in general. This method utilizes a computer (does not use a physical model), so the whole process can be carried out quickly, flexibly, inexpensively, and in-depth. It is not risky for cases related to human interaction. However, most researchers and engineers are still skeptical or doubtful about the results of this CFD simulation because of a lack of operational knowledge. However, sufficient theory is needed to make the correct simulation settings, so the concern is that the results can be more accurate. The credibility of the CFD simulation was determined based on the levels of uncertainty and error. The values of these uncertainties and errors were obtained through verification and validation.

The self-verification assessment determines whether the program and computations used for the created model are fundamentally correct. The validation determines whether the simulation follows the realities of the modeled physical case. Generally, validation is carried out using experimental methods or referring to similar previous studies. There is some disagreement among professionals regarding the standard procedure for verifying and validating CFD simulations. The detailed information from the overall simulation modeling of this work is presented in Table 1.

2.3. Validation and verification

One method to validate and verify a simulation is to focus on its convergence value. A value has converged if the graph has formed a straight line or the data has produced a constant value. When the iteration process continued, the value did not change. Convergence is one requirement for completing numerical simulations, which produces solutions of algebraic equations with values closest to the actual solutions of the partial differentials with the same initial and boundary conditions as the convergence mesh system. Three methods are commonly used to check the degree of convergence of the iteration results:

2.3.1. Convergence criteria

A calculation is initially said to have converged when the residual value is equal to zero; however, because it is difficult to achieve this state, ANSYS Fluent sets the convergence criterion at its default state, where the calculation stops when the iteration has produced a residual value that reaches that number. The default state of this simulation process has a residual value of 10–3 for almost all equations, except for the energy and radiation equations, which have a value of 10–6.

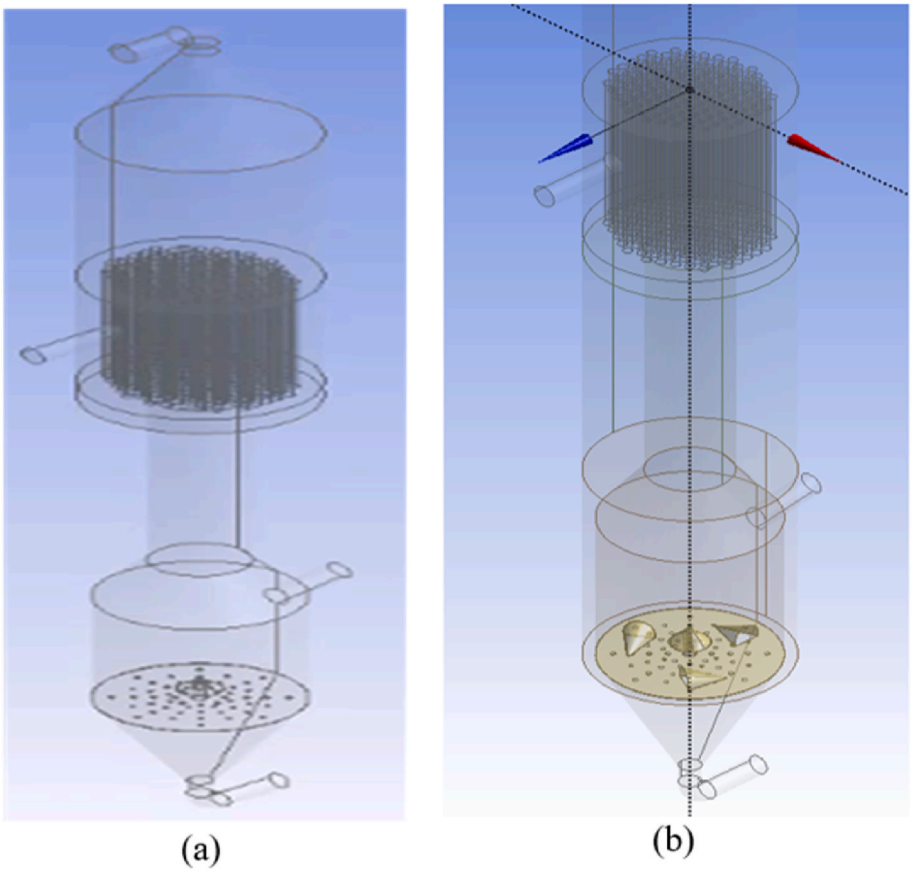

Fig. 3. (a) Model of standar plates (b) Model of modification plate.

Table 1
Detailed mesh model information.

	Geometry	Information of Mesh					
		Total		*Skewness*			
		Element	Nodes	Average	Maximum	Minimum	Remark
Model Mesh	1	1389859	325897	0.23747	0.84592	9.19E-06	Excellent
	2	1389560	326103	0.24038	0.8766	9.19E-06	Excellent

2.3.2. Monitor point

It is still challenging to achieve this when reaching the convergence point set by ANSYS Fluent, where the residual value does not want to fall again toward the predetermined convergence criteria. When the value of the continuous variable that predominantly represents the overall flow remains relatively unchanged when the iteration continues, the solution generated in that iteration can be said to be convergent.

2.3.3. Equilibrium

Mass, energy, momentum, and other quantities were balanced. To calculate the balance value between mass, energy, momentum, and other values in the Flux Report panel, in this case, use (**eq. (7)**). The results were considered convergent when the heat and mass balances of the total yield were less than 10% of the most negligible flux through the domain boundary.

$$\%\ different = \frac{the\ difference\ between\ the\ total\ inlet\ and\ outlet}{total\ inlet} \quad (7)$$

3. Results and discussion

This simulation was built to predict the combustion temperature when the perforated plate modification was applied to fluidized-bed combustor (FBC) technology with different fuels. This simulation aims to monitor whether FBC technology has achieved complete combustion. In addition, the amount and type of fuel used were also checked to determine the compatibility between the equipment and materials used. Complete combustion can be achieved when the fuel is burned out and nothing is left. The temperature obtained from this simulation was compared with the experimental results using FBC technology. The temperature observed in this simulation was based on a perforated plate or a geometry modeled with different fuels. The simulation results discussed in this work involved geometry modeling of one and three by testing three different variations.

3.1. Computation settings

The simulation was carried out using CFD software. The following are the computational settings used in this simulation to obtain the results of burning the coal in the boiler.

3.1.1. Gravity (−9.81 m/s)

3.1.1.1. Models.

- The fluid model used is Realizable to Standard Wall Function because it is accurate and often used in combustion simulations.
- Energy Equation (On)
- Discrete Phase (On)
- Radiation (On)
- The species (transport-reaction) eddy dissipation type with fuel specifications are shown in Table 2.

Table 2
Specification of fuel.

Proximate Analysis		Ultimate Analysis	
Volatile	0.727108	C	0.685185
Fixed Carbon	0.207156	H	0.095295
Ash	0.011257	O	0.21011
Moisture	0.054478	N	0.002002
		S	0.007407

Table 3
Boundary conditions.

Fuel Type	Fuel Calorific Value	Primary air-inlet	Fuel-Inlet
PKS	2.01 MJ	0.025 kg/kg_fuel	0.000833333 kg/s_fuel
OPM	1572 MJ	0.025 kg/kg_fuel	0.000833333 kg/s_fuel
EFB	1872 MJ	0.025 kg/kg_fuel	0.000833333 kg/s_fuel

3.2. Counter of temperature

The CFD simulation tested at this stage was conducted to investigate the temperature of the two types of geometries with variations in three different fuel types. The first simulation was tested for geometry-1 for each fuel and continued with geometry-2 for the same fuel type. The average temperature obtained from the simulation results in geometry-1 was recorded for OPM fuel at 2012 °C. The average temperatures for the EFB and PKS fuels were 1858 °C and 562 °C, respectively. Geometry-2 simulation results showed that the highest average temperature of the OPM fuel was 2031 °C.

Meanwhile, the average temperature recorded for each fuel was EFB 1985 °C and EFB 709 °C. Each simulation was performed using the same fuel and air intake, as shown in Table 3. Contour views of geometry-1 and geometry-2 with different fuel variations are presented in Fig. 4. Modifying the plate modeled in geometry-2 can increase the temperature compared with that before the modification in geometry-1. The simulation results are similar to the experimental results, where the plate modification applied to the fluidized-bed combustor technology can increase the temperature.

Overall, the simulation results performed on geometry-1 and geometry-2 show that the recorded temperature of the OPM fuel is higher. Meanwhile, PKS fuel, simulated in both geometries, produces lower temperatures. The low temperature of the PKS simulation is due to the properties of the ingredients in it, so the combustion is slower than OPM and EFB. The combustion properties of PKS during direct combustion experiments also burn slower than OPM and EFB. However, PKS fuel is suitable for direct combustion because it has a higher energy value and a longer burning time than OPM and EFB. While the results of direct combustion of OPM and EFB are also very easy to burn because they contain a lot of cellulose compared to PKS, thus, the combustion system shown in this simulation is in line with the properties of direct combustion.

3.3. Countur of velocity

A combustion simulation can be said to run well, which is determined by the speed of movement of the particles at a time. The particle

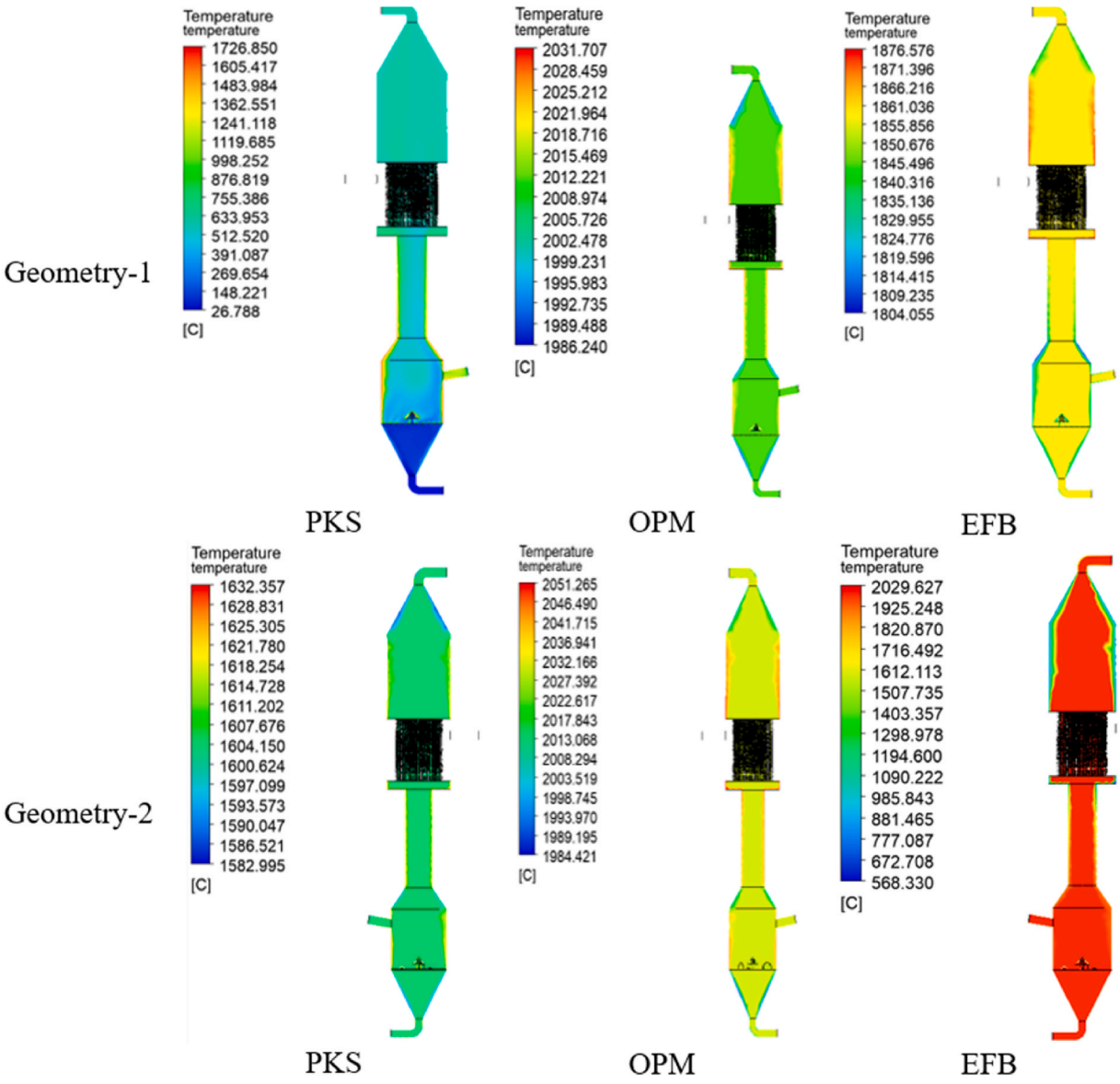

Fig. 4. Countur for the temperature at different fuel and geometries.

displacement velocity is essential in the simulation so that the expected temperature can be appropriately achieved and complete combustion can be achieved. The simulation results in this work show that the average velocity of OPM fuel particles for geometry-1 is 23.142 m/s. The average speed obtained from each fuel is PKS 22.226 m/s and EFB 20.55 m/s. The average particle displacement velocity at a time shown in geometry-2 is the highest recorded from PKS fuel, reaching 20.375 m/s. Meanwhile, the average speeds obtained from OPM and EFB fuel are 20.124 m/s and 19.057 m/s. The particle displacement velocity contours obtained from the simulation results are shown in Fig. 5.

Air velocity in the combustion chamber is one of the most important in combustion, directly or through simulation. The appropriate air velocity in the combustion chamber will result in complete combustion. Based on the results of the simulations carried out for each case, the air velocity during the simulation with PKS fuel for geometry-1 is higher. Hence, the resulting temperature is also higher. While the airspeed obtained from PKS is slightly higher than EFB for geometry-1. However, the temperature obtained from EFB is higher than PKS. This is due to the delay in PKS burning, so the resulting temperature is lower. While the air velocity recorded from PKS in geometry-2 is slightly higher, the delay in combustion that occurs in PKS results in a lower temperature. This simulation uses the same time and fuel weight for each fuel tested.

3.4. Countur of carbon monoxide

Fig. 6 shows a carbon monoxide (CO) contour display from the simulation results for each variation and geometry. The highest CO values recorded in geometry-1 for each fuel were 9.27% for PKS, 5.41% for OPM, and 2.26% for EFB. The maximum CO values obtained from the geometry-2 simulation results were PKS 5.79%, OPM 3.80%, and EFB 1.92%. Modifying the plate modeled in geometry-2 can reduce the CO compared to the simulation with geometry-1 without any plate modification. The highest CO reduction was from the PKS fuel at 3.48%, OPM 1.61%, and EFB 0.34%.

Based on the analysis results from the simulations carried out on geometry-1 and geometry-2, EFB and OPM fuels produce lower CO than PKS. In addition, modification of geometry-2 in the combustion chamber can also reduce CO for all cases tested in this study. Thus, modifying the plate modeled in the combustion chamber can give better results than the standard plate.

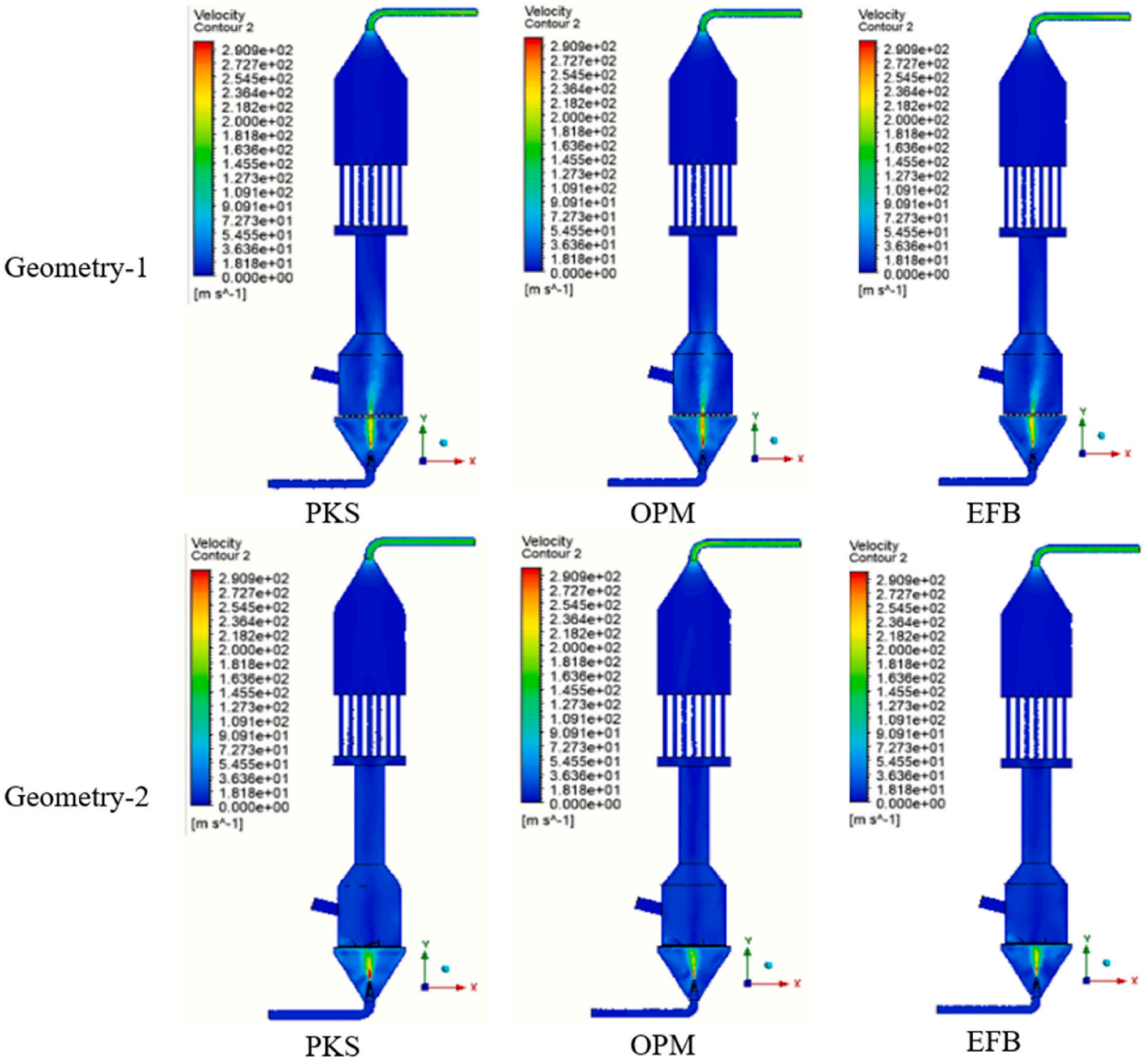

Fig. 5. Velocity at different fuel and geometries.

3.5. Countur of hydrogen

The analysis of the simulation results carried out at this stage was the amount of carbon dioxide from the combustion of different fuels through CFD modeling. The H_2O contours for each fuel from geometries 1 and 2 are presented in Fig. 7. The simulation results for geometry-1 tested with PKS fuel can produce a maximum H2O value of 0.022%. Meanwhile, the maximum yields of H_2O from OPM and EFB fuel during the simulation in geometry-1 reached 0.017% and 0.017%, respectively. Furthermore, simulations were carried out for geometry-2 by applying various modifications to the same fuel during the geometry-1 test.

Based on the results of simulations carried out with PKS fuel, 0.022% H2O can be produced. The maximum values of H_2O recorded during the simulation using OPM and EFB were 0.041% and 0.032%, respectively. Based on the results of the investigations, the OPM and EFB fuels showed a slight increase when there was a plate modification contained in geometry-2. However, the PKS fuel is slightly reduced when the perforated plate modification is applied in geometry-2 modeling.

3.6. Countur of oxygen

An analysis of the simulation results at this stage was carried out to investigate the average value of O_2 from different fuels to the geometry with and without modification. A high concentration of O_2 indicates a decrease in combustion temperature and vice versa. When the temperature was increased, O_2 decreased. The simulation results for geometry-1 without modification of each fuel showed an average O_2 concentration of PKS 0.163 (16%), OPM 0.179 (18%), and EFB 0.166 (17%). The maximum O_2 values obtained from the geometry-1 simulation for each fuel are PKS 0.166 (17%), 0.179 (18%), and 0.166 (17%). The average O_2 concentration level from the simulation results using PKS fuel was slightly lower than those of OPM and EFB.

The simulation results performed on geometry-2 with the same fuel as geometry-1 showed average O_2 values of 0.178 (18%), 0.148 (15%), and 0.143 (14%), respectively. As for the maximum O_2 values from the results of the geometry-2 simulation, the PKS was 0.178 (18%), OPM was 0.149 (15%), and EFB was 0.143 (14%). The simulation results for geometry-2 show that the average O_2 value of the PKS fuel increased slightly compared to the simulation results for geometry-1. However, the temperature obtained from geometry-2 was higher, as shown by the contour in Fig. 4. The OPM and EFB fuel from the geometry-2 simulation decreased compared with the simulation in geometry-1. The O_2 contour display obtained from the simulation results for geometry-2 is shown in Fig. 8.

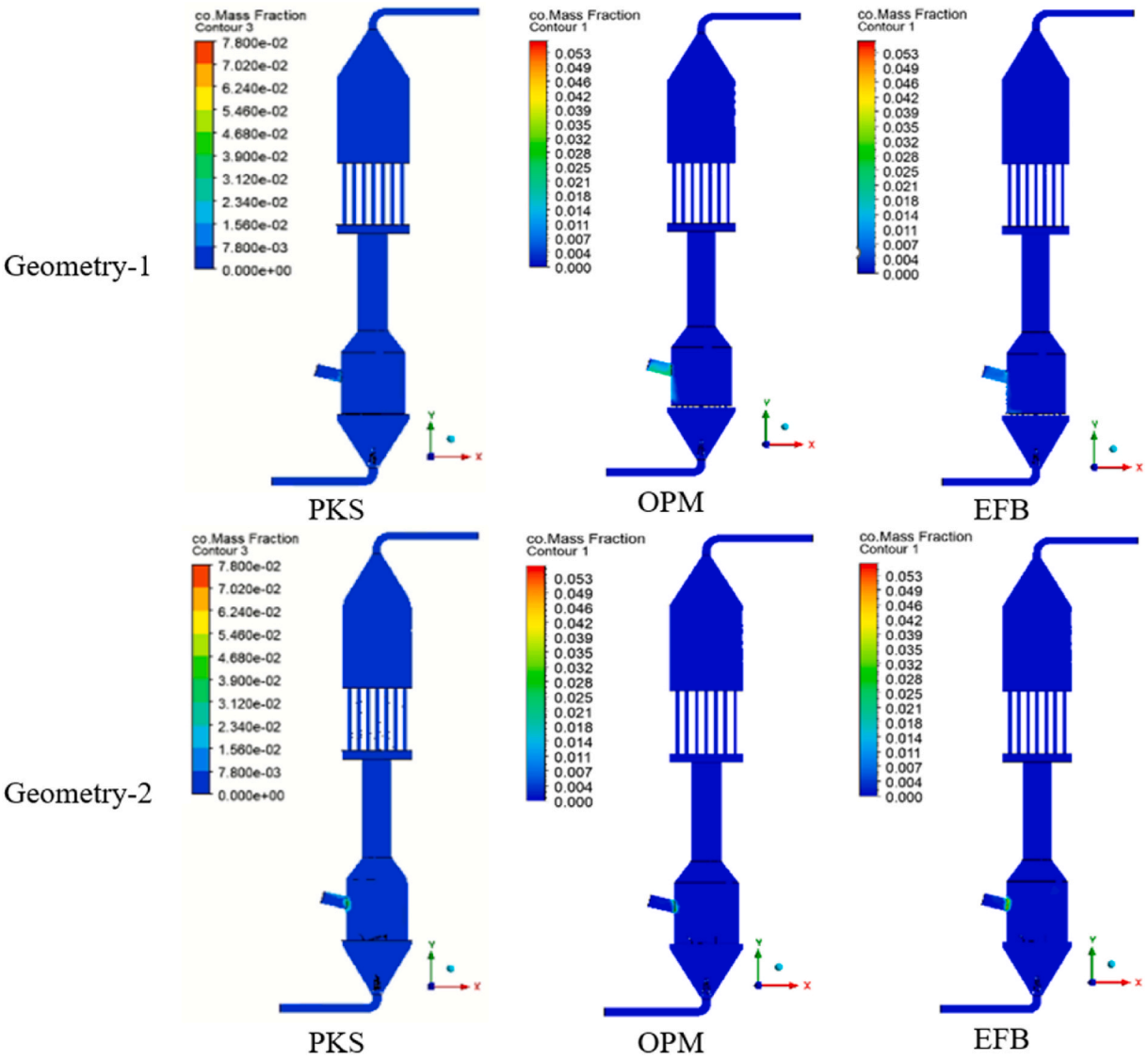

Fig. 6. CO at different fuel and geometries.

A comparison of boiler efficiency from the simulation results with geometry-1 without modification and modified geometry-2 with PKS, OPM, and EFB fuel in full is presented in Table 4. Geometric modeling was performed with the same surface area and amount of fuel for each type of fuel tested. Based on the simulation analysis results, the best boiler efficiency was obtained from the OPM fuel of 34%. While the highest calorific value was recorded for PKS fuel, the boiler efficiency during the simulation with PKS fuel was lower than that of OPM and EFB.

The radiation values obtained from the simulation results of the two geometries with different fuels are listed in Table 5. The highest radiation simulation results on geometry-1 were recorded for PKS fuel, which reached 85.280 W/m^2 with heat loss during the simulation process of approximately 2.17 W/m^2. However, when the simulation used geometry-2 with modifications, it decreased compared to 1.70 W/m^2 with a heat loss rate of approximately 1.95 W/m^2. The EFB fuel tested by simulation using geometry-2 showed a significant increase of 90.889 W/m^{2,} with a heat loss rate of 1.91 W/m^2. Meanwhile, the OPM fuel tested in the geometry-2 simulation also experienced a slight decrease to 44.466 W/m^2 from 62.255 W/m^2 obtained from geometry-1. The combustion temperature determines the increase in the radiation from each fuel used. The higher the temperature and lower the heat loss, so the more increase in radiation in the combustion chamber.

The CFD simulation carried out in this study validated data from laboratory-scale experiments. The combustion chamber of the FBC technology can only accommodate 3 kg of fuel, especially for OPM and EFB. All values entered are constant, so results are more visible than larger fuel inputs. Although the simulation in this work uses less fuel input, the results are not much different from more fuel input. However, the primary purpose of the simulation through modeling is to evaluate the temperature level with plate modification in geometry. The simulation results show the plate modification on the floor, where the fuel can increase the temperature. These results are also the same as those of the experiments conducted, where the plate modifications applied in the FBC technology combustion chamber than increased the temperature and radiation in the combustion chamber. Thus, future research, particularly simulations, must consider the amount of fuel input to obtain more optimal results.

The simulation data analysis results show that modifying the perforated plate modeled through geometry-2 can increase the temperature by about 147 °C compared to the standard plate or geometry-2, especially for PKS fuel. Meanwhile, OPM and EFB fuel increased by 19 °C and 127 °C, respectively. In addition, the effect of modification of the perforated plate (geometry-2) can also reduce CO_2 0.019 P KS, 0.025

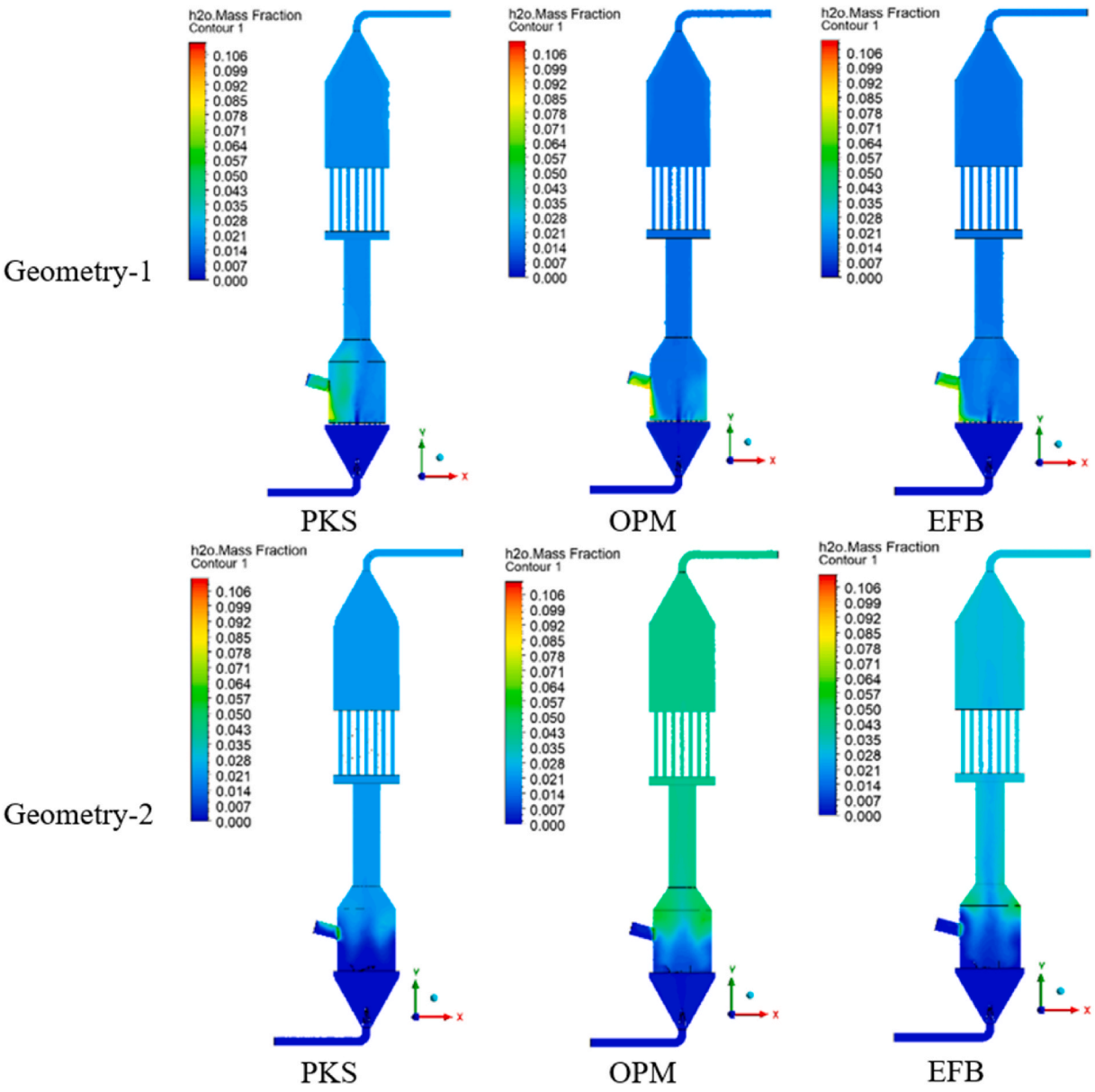

Fig. 7. H_2O at different fuel and geometries.

OPM, and 0.014 EFB, respectively. Meanwhile, O_2, H_2O, and speed increase when the simulation changes the perforated plate (geometry-2) compared to the standard plate (geometry-1). Comparison results of standard plates (geometry-1) and modified plates (geometry-2) are presented in Table 6.

The present study on the modification of a perforated plate in a fluidized-bed combustor chamber through computational fluid dynamics simulation has several practical implications. Firstly, the study can help in optimizing the performance of the fluidized-bed combustor chamber. By simulating different modifications to the perforated plate, the study can identify the design that provides the best fluidization and mixing of the fuel and air, leading to efficient combustion and reduced emissions. Secondly, the study can aid in reducing the environmental impact of fluidized-bed combustion. By optimizing the combustion process, the study can reduce the emissions of greenhouse gases and other pollutants, improving air quality and reducing the carbon footprint of the process. Thirdly, the study can provide valuable insights into the design and operation of fluidized-bed combustors. By using computational fluid dynamics simulations, the study can help to understand the complex fluid dynamics and heat transfer phenomena that occur in the combustor, leading to better designs and more efficient operation. Overall, the present study has practical implications for improving the performance, reducing the environmental impact, and advancing the design and operation of fluidized-bed combustors.

The simulation results can provide detailed information on various important aspects of the combustion process, including fluid flow characteristics, temperature distribution, gas composition, and chemical reaction rates. Following are some detailed interpretations that can be obtained from the CFD simulation results for solid fuel combustion:

1. Fluid Flow Characteristics: CFD simulation allows us to see the fluid flow patterns around solid fuels during combustion. This can assist in understanding air and fuel distribution, zones of turbulence, and any disturbances or changes in flow that may affect combustion efficiency.
2. Temperature Distribution: In the combustion process, temperature is an important parameter that affects the chemical reaction rate and combustion efficiency. CFD simulation can provide a detailed picture of the temperature distribution around solid fuels. This information is invaluable in understanding hot or cold zones, optimal burning

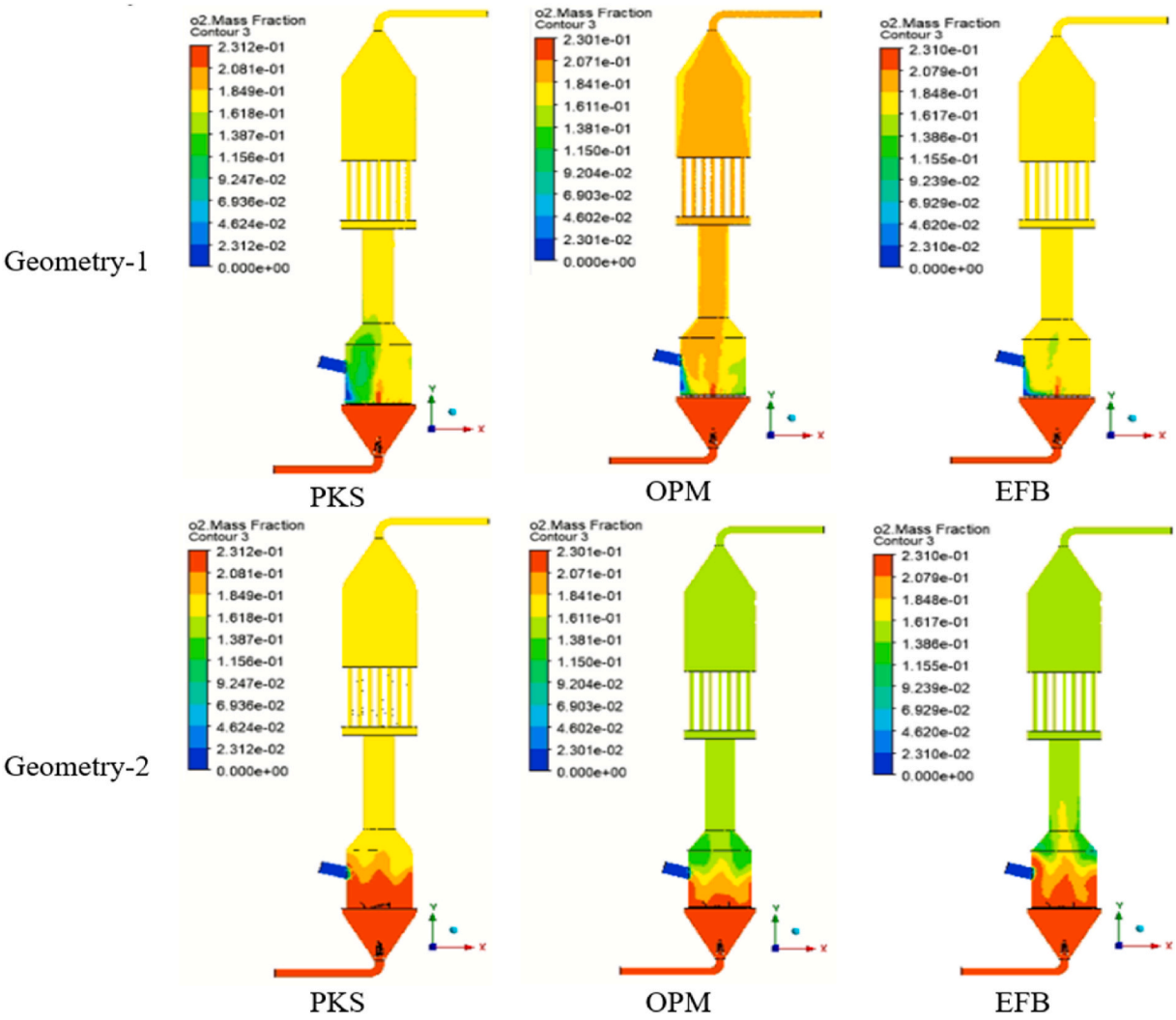

Fig. 8. O_2 at different geometries and variations.

Table 4
Comparison of boiler efficiency of different fuels.

Geometry	Fuel Type	Outlet surface area (m^2)	Heat flux (W/m^2)	Calorific value (J/kg)	Mass flow rate (kg/s)	Total of fuel (kg/s)	Efficiency boiler (%)
1	PKS	2.65	2.88	2.01	7.72	8.33	30
	OPM	2.65	1.66	1.57	7.78	8.33	34
	EFB	2.65	1.96	1.87	7.75	8.33	33
2	PKS	2.65	1.03	2.01	3.16	8.33	16
	OPM	2.65	1.25	1.57	7.32	8.33	25
	EFB	2.65	1.30	1.87	7.32	8.33	22

Table 5
Comparison of radiation and Heat loss with three different variations.

Geometry	Fuel Type	Max radiation (W/m^2)	Heat Loss (W)
1	PKS	85.280	2.17
	OPM	62.255	1.75
	EFB	1.42	2.08
2	PKS	1.70	1.95
	OPM	44.466	1.64
	EFB	90.889	1.91

areas, and the risk of unwanted conditions such as hotspots or incomplete combustion.

3. Gas Composition: Apart from temperature, CFD simulation can also provide insight into the gas composition within the combustion zone. This is closely related to the availability of oxygen and the chemical changes that occur during the combustion of solid fuels. By understanding the gas composition distribution, we can analyze the efficient combustion rate, the presence of unwanted by-products, and the relevant emission parameters.
4. Chemical Reaction Rates: CFD Simulation allows us to model and predict the rates of chemical reactions that occur during the combustion of solid fuels. This information can assist in optimizing the combustion system design, including fuel selection, air-fuel mixture ratio, and airflow control, to achieve high combustion efficiency and reduce pollutant emissions.
5. Combustion Efficiency and Emissions: CFD simulation results can provide an in-depth understanding of the combustion efficiency of solid fuels, including complete or incomplete combustion. In

Table 6
Comparison results between standard plates and plate modifications.

Geometry	Mass Fraction CO%	Mass Fraction CO_2%	Mass Fraction O_2%	Mass Fraction H_2O%	Temperature ^oC	Velocity [m/s]
1	9.27	0.053	0.163	0.021	562	22.226
	5.41	0.051	0.179	0.017	2012	23.142
	2.26	0.048	0.166	0.018	1858	20.55
2	5.79	0.034	0.185	0.022	709	24.756
	3.80	0.026	0.200	0.041	2031	26.864
	1.92	0.034	0.186	0.032	1985	23.343

addition, this simulation can also reveal estimates of pollutant emissions such as particulate matter, exhaust gases, and other toxic compounds. This information is invaluable in developing strategies for reducing emissions and increasing the efficiency of combustion processes.

4. Conclusions and prospects

The simulation through CFD modeling tested in this study was carried out on two geometries with three different fuel type variations. Based on the results of the simulation that has been carried out, several conclusions can be drawn as follows:

1. Geometry modeling by modifying the fuel floor can increase the temperature compared to that before the modification.
2. The best efficiency was obtained from geometry-1 for the OPM fuel at 34%, and the lowest efficiency of 16% was recorded for the PKS fuel for geometry-2.
3. The highest radiation was recorded from the simulation results with geometry-2 for EFB fuel at 90.889 W/m^2 with an energy loss rate of 1.91 W/m^2. Meanwhile, the highest radiation generated from the geometry-1 simulation was 85.280 $W/m^{2,}$ with a level heat loss of approximately 2.17 W/m^2.

This simulation test was carried out to investigate the temperature, radiation, and heat loss profiles of three types of solid fuel with different geometries. This simulation was carried out to validate the experimental results, but the simulation results through the steady state did not show optimal results. Thus, to validate the results of further experiments can be done with transient simulations. This is because during the experiment, it is dynamic (using time), so it is more suitable for simulation with transients.

4.1. Prospects

Investigations through CFD simulations carried out in this study only arrived at validating the combustion properties of the three fuel types used during the experiment. Simulation in this work to see the temperature, air speed, air density, radiation, and fuel combustion speed PKS, OPM, and EFB. Meanwhile, for the analysis and validation of the data as a whole, it is still working on further analysis. In addition, the analysis and prediction of the energy produced from each fuel for each case is also in the process of future work.

The use of computational fluid dynamics (CFD) simulations to study the performance of fluidized-bed combustors is a growing area of research in the field of energy engineering. Perforated plates are commonly used in fluidized-bed combustors to distribute air evenly and maintain a stable combustion process. CFD simulations can be used to study the effects of different modifications to the perforated plate design, such as changes in the hole diameter, spacing, and pattern. By analyzing the fluid dynamics within the combustor chamber, CFD simulations can predict the impact of these modifications on combustion efficiency, emissions, and other performance parameters.

In the future, there are several prospects for the use of CFD simulations to optimize the design of perforated plates in fluidized-bed combustors. For example, CFD simulations can be used to study the effects of different operating conditions, such as fuel properties, temperature, and pressure, on the performance of the combustor. Furthermore, advances in CFD software and computing technology will allow for more detailed and accurate simulations of fluidized-bed combustors. This will enable researchers to study the behaviors of combustion processes at a finer scale, leading to more precise predictions of the effects of different modifications to the perforated plate design. Overall, the prospects for the use of CFD simulations to optimize the design of perforated plates in fluidized-bed combustors are promising and will continue to be an important area of research in the field of energy engineering.

Credit author statement

Erdiwansyah: Data curation, Writing- Original draft preparation. Mahidin and Asri Gani: Supervision, Conceptualization, Methodology, Software, Visualization, Investigation. Husni Husin: Supervision, Visualization. Nasaruddin: Supervision, Software, Validation.: Rizalman Mamat:Writing- Reviewing and Editing.

Declaration of competing interest

The authors declare that they have no known competing financial interests or personal relationships that could have appeared to influence the work reported in this paper.

Data availability

No data was used for the research described in the article.

Acknowledgments

This research was supported by Universitas Syiah Kuala, Research institutions, and community services with contract numbers (166/UN11/SPK/PNBP/2021), Research Grant (RDU223310) from Universiti Malaysia Pahang (UMP), and Badan Pengelola Dana Perkebunan Kelapa Sawit (BPDPKS) with grant number (PRJ-374/DPKS/2022 and 1269/UN 11.2.1/HK.00.07/2022).

Nomenclature

CFD	Computational fluid dynamics
PKS	Palm kernel shell
OPM	Oil palm midrib
EFB	Empty fruit bunches
FBC	Fluidized-bed combustor
CO_2	Carbon dioxide
CO	Carbon monoxide
H_2O	Hydrogen
O_2	Oxygen
^oC	Degree celcius
W/m^2	Watt meter kuadrat
W	Watt
m/s	Meter per second
J/kg	Joule per kilo gram

Kg/s	Kilo gram per second
C	Carbon
H	Hydrogen
O	Oxygen
N	Nitrogen
S	Sulfur

References

[1] J. Sánchez, M.D. Curt, N. Robert, J. Fernández, Chapter two - biomass resources, in: C. Lago, N. Caldés (Eds.), Y.B.T.-T.R. of B. in the B. Lechón, Academic Press, 2019, pp. 25–111, https://doi.org/10.1016/B978-0-12-813056-8.00002-9.

[2] J. Islas, F. Manzini, O. Masera, V. Vargas, Chapter four - solid biomass to heat and power, in: C. Lago, N. Caldés (Eds.), Y.B.T.-T.R. of B. in the B. Lechón, Academic Press, 2019, pp. 145–177, https://doi.org/10.1016/B978-0-12-813056-8.00004-2.

[3] R. Mamat M.S.M. Sani K. Sudhakar Erdiwansyah, Renewable energy in southeast asia: policies and recommendations, Sci. Total Environ. (2019), https://doi.org/10.1016/j.scitotenv.2019.03.273.

[4] T. Jarunglumlert, A. Bampenrat, H. Sukkathanyawat, P. Pavasant, C. Prommuak, Enhancing the potential of sugarcane bagasse for the production of ENplus quality fuel pellets by torrefaction: an economic feasibility study, Biofuel Res. J. 9 (2022) 1707–1720.

[5] D. Patiño, R. Pérez-Orozco, J. Porteiro, M. Lapuerta, Characterization of biomass PM emissions using thermophoretic sampling: composition and morphological description of the carbonaceous residues, J. Aerosol Sci. 127 (2019) 49–62, https://doi.org/10.1016/j.jaerosci.2018.10.005.

[6] J.J. Rico, R. Pérez-Orozco, N. Cid, A. Larrañaga, J.L. Míguez Tabarés, Viability of agricultural and forestry residues as biomass fuels in the Galicia-North Portugal Region: an experimental study, Sustainability 12 (2020) 8206.

[7] S. Chapela, J. Porteiro, M.A. Gómez, D. Patiño, J.L. Míguez, Comprehensive CFD modeling of the ash deposition in a biomass packed bed burner, Fuel 234 (2018) 1099–1122, https://doi.org/10.1016/j.fuel.2018.07.121.

[8] S. Chapela, J. Porteiro, M. Garabatos, D. Patiño, M.A. Gómez, J.L. Míguez, CFD study of fouling phenomena in small-scale biomass boilers: experimental validation with two different boilers, Renew. Energy 140 (2019) 552–562, https://doi.org/10.1016/j.renene.2019.03.081.

[9] Y. Cai, K. Tay, Z. Zheng, W. Yang, H. Wang, G. Zeng, Z. Li, S. Keng Boon, P. Subbaiah, Modeling of ash formation and deposition processes in coal and biomass fired boilers: a comprehensive review, Appl. Energy 230 (2018) 1447–1544, https://doi.org/10.1016/j.apenergy.2018.08.084.

[10] S. Chapela, N. Cid, J. Porteiro, J.L. Míguez, Numerical transient modelling of the fouling phenomena and its influence on thermal performance in a low-scale biomass shell boiler, Renew. Energy 161 (2020) 309–318, https://doi.org/10.1016/j.renene.2020.07.068.

[11] S. Chapela, J. Porteiro, J.L. Míguez, F. Behrendt, Eulerian CFD fouling model for fixed bed biomass combustion systems, Fuel 278 (2020), 118251, https://doi.org/10.1016/j.fuel.2020.118251.

[12] A. Regueiro, D. Patiño, J. Porteiro, E. Granada, J.L. Míguez, Effect of air staging ratios on the burning rate and emissions in an underfeed fixed-bed biomass combustor, Energies 9 (2016) 940.

[13] Mahidin Erdiwansyah, H. Husin, M. Faisal, Muhtadin, A. Gani, R.E. Sardjono, R. Mamat, The modification of the perforated plate in the fluidized-bed combustor to analyze heat convection rate and temperature, J. Combust. 2021 (2021), 4084162, https://doi.org/10.1155/2021/4084162.

[14] H. Khodaei, F. Guzzomi, D. Patiño, B. Rashidian, G.H. Yeoh, Air staging strategies in biomass combustion-gaseous and particulate emission reduction potentials, Fuel Process. Technol. 157 (2017) 29–41, https://doi.org/10.1016/j.fuproc.2016.11.007.

[15] G. Archan, A. Anca-Couce, M. Buchmayr, C. Hochenauer, J. Gruber, R. Scharler, Experimental evaluation of primary measures for NOX and dust emission reduction in a novel 200 kW multi-fuel biomass boiler, Renew. Energy 170 (2021) 1186–1196, https://doi.org/10.1016/j.renene.2021.02.055.

[16] E. Erdiwansyah, M. Mahidin, H. Husin, N. Nasaruddin, A. Gani, M. Faisal, M. Muhtadin, M. Zaki, R. Mamat, Comparison of temperature, radiation rate, heat loss, furnace and thermal efficiencies of different plates in the FBC combustion chamber, Front. Heat Mass Transf. 20 (2023).

[17] R. Pérez-Orozco, D. Patiño, J. Porteiro, J.J. Rico, The effect of primary measures for controlling biomass bed temperature on PM emission through analysis of the generated residues, Fuel 280 (2020), 118702, https://doi.org/10.1016/j.fuel.2020.118702.

[18] R. Perez-Orozco, D. Patino, J. Porteiro, A. Larranaga, Flue gas recirculation during biomass combustion: implications on PM release, Energy Fuel. 34 (2020) 11112–11122.

[19] M.A. Gómez, R. Martín, S. Chapela, J. Porteiro, Steady CFD combustion modeling for biomass boilers: an application to the study of the exhaust gas recirculation performance, Energy Convers. Manag. 179 (2019) 91–103, https://doi.org/10.1016/j.enconman.2018.10.052.

[20] M. Gehrig, S. Pelz, D. Jaeger, G. Hofmeister, A. Groll, H. Thorwarth, W. Haslinger, Implementation of a firebed cooling device and its influence on emissions and combustion parameters at a residential wood pellet boiler, Appl. Energy 159 (2015) 310–316, https://doi.org/10.1016/j.apenergy.2015.08.133.

[21] M. Gehrig, D. Jaeger, S.K. Pelz, R. Kirchhof, H. Thorwarth, W. Haslinger, Influence of a direct firebed cooling in a residential wood pellet boiler with an ash-rich fuel on the combustion process and emissions, Energy Fuel. 30 (2016) 9900–9907.

[22] R. Pérez-Orozco, D. Patiño, J. Porteiro, J.L. Míguez, Novel test bench for the active reduction of biomass particulate matter emissions, Sustainability 12 (2020) 422.

[23] R. Pérez-Orozco, D. Patiño, J. Porteiro, J.L. Míguez, Bed cooling effects in solid particulate matter emissions during biomass combustion, A morphological insight, Energy. 205 (2020), 118088, https://doi.org/10.1016/j.energy.2020.118088.

[24] F. Zhao, A. Wei, Q. Chen, Y. Song, S. Wu, X. Zhang, Performance analysis of double-stage perforated plate flowmeter for cryogenic fluids, Cryogenics 124 (2022), 103485, https://doi.org/10.1016/j.cryogenics.2022.103485.

[25] D. Kim, Y. Won, S.Y. Park, J.-H. Choi, J.B. Joo, S.-H. Jo, Rate of CO2 adsorbent attrition induced by gas jets on perforated plate distributors in bubbling fluidized beds, Adv. Powder Technol. 31 (2020) 4411–4419, https://doi.org/10.1016/j.apt.2020.09.015.

[26] Y. Bayazit, E.M. Sparrow, D.D. Joseph, Perforated plates for fluid management: plate geometry effects and flow regimes, Int. J. Therm. Sci. 85 (2014) 104–111, https://doi.org/10.1016/j.ijthermalsci.2014.06.002.

[27] F. Chen, Z. Jin, Effects of perforated plate on hydrogen flow in L-shaped high pressure reducing valve, Int. J. Hydrogen Energy 48 (2023) 1956–1967, https://doi.org/10.1016/j.ijhydene.2022.09.276.

[28] R. Scharler, T. Gruber, A. Ehrenhöfer, J. Kelz, R.M. Bardar, T. Bauer, C. Hochenauer, A. Anca-Couce, Transient CFD simulation of wood log combustion in stoves, Renew. Energy 145 (2020) 651–662, https://doi.org/10.1016/j.renene.2019.06.053.

[29] T. Zadravec, B. Rajh, F. Kokalj, N. Samec, CFD modelling of air staged combustion in a wood pellet boiler using the coupled modelling approach, Therm. Sci. Eng. Prog. 20 (2020), 100715, https://doi.org/10.1016/j.tsep.2020.100715.

[30] M. Buchmayr, J. Gruber, M. Hargassner, C. Hochenauer, A computationally inexpensive CFD approach for small-scale biomass burners equipped with enhanced air staging, Energy Convers. Manag. 115 (2016) 32–42, https://doi.org/10.1016/j.enconman.2016.02.038.

[31] J. Wiese, F. Wissing, D. Höhner, S. Wirtz, V. Scherer, U. Ley, H.M. Behr, DEM/CFD modeling of the fuel conversion in a pellet stove, Fuel Process, Technol. 152 (2016) 223–239, https://doi.org/10.1016/j.fuproc.2016.06.005.

[32] S. Somwangthanaroj, S. Fukuda, CFD modeling of biomass grate combustion using a steady-state discrete particle model (DPM) approach, Renew. Energy 148 (2020) 363–373, https://doi.org/10.1016/j.renene.2019.10.042.

[33] M.A. Gómez, J. Porteiro, D. Patiño, J.L. Míguez, Eulerian CFD modelling for biomass combustion. Transient simulation of an underfeed pellet boiler, Energy Convers. Manag. 101 (2015) 666–680, https://doi.org/10.1016/j.enconman.2015.06.003.

[34] A. Rezeau, L.I. Díez, J. Royo, M. Díaz-Ramírez, Efficient diagnosis of grate-fired biomass boilers by a simplified CFD-based approach, Fuel Process. Technol. 171 (2018) 318–329, https://doi.org/10.1016/j.fuproc.2017.11.024.

[35] C.A. Bermúdez, J. Porteiro, L.G. Varela, S. Chapela, D. Patiño, Three-dimensional CFD simulation of a large-scale grate-fired biomass furnace, Fuel Process. Technol. 198 (2020), 106219, https://doi.org/10.1016/j.fuproc.2019.106219.

[36] M.R. Karim, A.A. Bhuiyan, J. Naser, Effect of recycled flue gas ratios for pellet type biomass combustion in a packed bed furnace, Int. J. Heat Mass Tran. 120 (2018) 1031–1043, https://doi.org/10.1016/j.ijheatmasstransfer.2017.12.116.

[37] M.R. Karim, A.A. Bhuiyan, A.A.R. Sarhan, J. Naser, CFD simulation of biomass thermal conversion under air/oxy-fuel conditions in a reciprocating grate boiler, Renew. Energy 146 (2020) 1416–1428, https://doi.org/10.1016/j.renene.2019.07.068.

[38] M.R. Karim, J. Naser, CFD modelling of combustion and associated emission of wet woody biomass in a 4 MW moving grate boiler, Fuel 222 (2018) 656–674, https://doi.org/10.1016/j.fuel.2018.02.195.

[39] H. Sefidari, N. Razmjoo, M. Strand, An experimental study of combustion and emissions of two types of woody biomass in a 12-MW reciprocating-grate boiler, Fuel 135 (2014) 120–129, https://doi.org/10.1016/j.fuel.2014.06.051.

[40] M.A. Gómez, J. Porteiro, D. Patiño, J.L. Míguez, CFD modelling of thermal conversion and packed bed compaction in biomass combustion, Fuel 117 (2014) 716–732, https://doi.org/10.1016/j.fuel.2013.08.078.

[41] L.G. Varela, C.Á. Bermúdez, S. Chapela, J. Porteiro, J.L.M. Tabarés, Improving bed movement physics in biomass computational fluid dynamics combustion simulations, Chem. Eng. Technol. 42 (2019) 2556–2564.

[42] Mahidin Erdiwansyah, H. Husin, Muhtadin Nasaruddin, M. Faisal, A. Gani, Usman, R. Mamat, Combustion efficiency in a fluidized-bed combustor with a modified perforated plate for air distribution, Processes 9 (2021), https://doi.org/10.3390/pr9091489.

[43] E. Erdiwansyah, M. Mahidin, H. Husin, M. Faisal, U. Usman, M. Muhtadin, A. Gani, R. Mamat, Modification perforated plate in the fluidize-bed combustor to investigation of heat convection rate and temperature, Front. Heat Mass Transf. 18 (2022).

[44] M. Mahidin, H. Hamdani, H. Hisbullah, E. Erdiwansyah, M. Muhtadin, M. Faisal, U. Usman, N.A.C. Sidik, Experimental on the FBC chamber for analysis temperature and combustion efficiency using palm oil biomass fuel, Trans. Can. Soc. Mech. Eng. 46 (2022).